



# Narrow-band, Bragg-grating-assisted Microring Reflectors: Tunability, Reflection Loss and Group Delay

Carmen Vázquez, and Otto Schwelb\*

Departamento Tecnología Electrónica, Universidad Carlos III, Leganés 28911, Madrid, SPAIN  
Tel: +34.91.624.9191; Fax: +34.91.624.9430; E-mail: [cvazquez@ing.uc3m.es](mailto:cvazquez@ing.uc3m.es)

\*Department of Electrical and Computer Engineering  
Concordia University, Montréal, Québec, H3G 1M8 CANADA  
Tel: +514.573.9155; Fax: +514.848.2802; E-mail: [otto@ece.concordia.ca](mailto:otto@ece.concordia.ca)

**Abstract**—Two configurations based on Bragg grating assisted single-ring microresonators are analyzed and simulated. Device characteristics such as bandwidth, sensitivity to loss, effect of external coupling, tunability and group delay are evaluated. The relationship between the resonator mode number and the grating parameters and the rules for selecting appropriate mode numbers are discussed. The dependence of reflection loss on waveguide attenuation and grating reflection coefficient illustrate the analytical results.

**Index Terms**—Bragg gratings, integrated optics, mirrors, optical resonators, optical waveguide components.

## I. INTRODUCTION

Microring resonator based optical mirrors and band-limited reflectors have been the subject of intense investigations in recent years, primarily due to the advancement in fabrication technology and miniaturization of integrated devices [1]-[6]. In this paper we present analytical and simulated results on the performance of two closely related narrow-band laser mirror configurations. Both consist of a microring resonator to which, through a coupler, two identical Bragg gratings are attached. The first configuration, illustrated schematically in Fig. 1a) has been discussed in a different context in [7]-[10] while the second configuration, shown in Fig. 1b), was briefly treated in [11]. Although they share similarities, their characteristics and fabrication differs in respects that could determine the choice of application. For example, Fig. 1a) indicates a coupler geometry connecting the resonator to the Bragg waveguides that might require vertical

coupling technology to avoid bends of very small radii causing excessive radiation loss. Other aspects differentiating the configurations are tunability, bandwidth, sensitivity to loss and the most convenient positioning of (thermo-optic) tuning pads.

In what follows we shall discuss the analytical aspects of treating these devices, including a circuit reduction scheme that simplifies the arithmetic, and present computed results for tuning sensitivity and for the effect of loss on reflected intensity and on group delay in reflection [12].

## II. ANALYSIS

Referring to Fig. 1,  $K$  represents the power coupling coefficient of the coupler between the resonator and the gratings, while the location of  $K$  within the ring, determined by  $h$  ( $0 < h < 1$ ), is arbitrary. All four transmission line sections, namely  $hL$ ,  $(1-h)L$ ,  $l_3$  and  $l_4$ , are characterized by the same effective refractive index  $n_{eff}$  and the same amplitude attenuation coefficient  $\alpha$ , although this restriction can easily be relaxed. We also admit localized or distributed gain in the ring [13]-[15] and thermo-optic length or refractive index adjustment [16] of  $L$ ,  $l_3$ ,  $l_4$  and  $n_{eff}$ . All lengths are given in terms of mode numbers, for example,  $N = Ln_{eff}/\lambda_0$ , where  $\lambda_0$  is the design wavelength. Another important parameter is the round trip time delay  $\tau_0 = N/f_0$ , where  $f_0$  is the design frequency. The gratings are identical, quarter wavelength shallow gratings, meaning that the relative index difference

$(n_b - n_a)/n_a \ll 1$ , and  $N_G$  is the number of periods. Balanced operation normally requires  $K \cong 0.5$ , whereas  $K_c$  is usually small to prevent loading and to preserve the resonance spectrum of the grating-assisted ring.

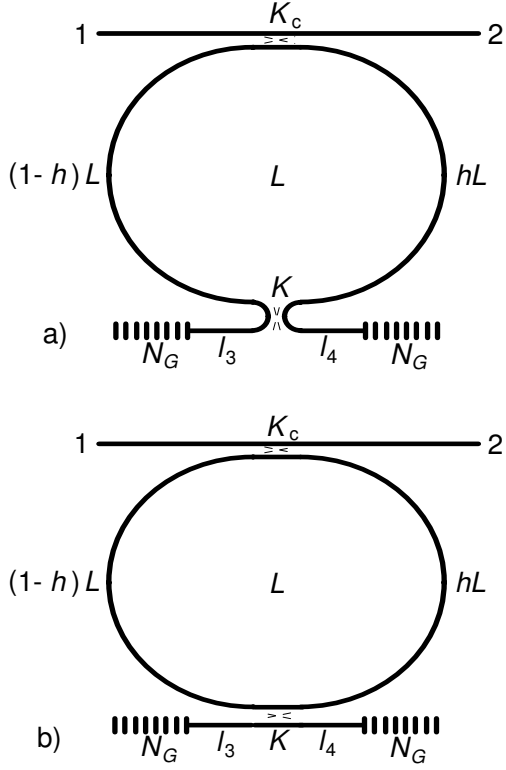


Fig.1. Two grating-assisted microring resonator laser mirrors. The ring perimeter is  $L$ ,  $h$  locates the coupler  $K$  on the ring. The ring need not be circular.

Figs. 1a) and 1b) can be simplified by combining the reflectors and the coupler  $K$  into a single two-port, characterized by its  $2 \times 2$  scattering matrix  $S_K$ , and embedding this two-port into the ring.  $S_K$  can be calculated from first principles and is found to be

$$S_K = \begin{bmatrix} c^2\Gamma_3 - s^2\Gamma_4 & jsc(\Gamma_3 + \Gamma_4) \\ jsc(\Gamma_3 + \Gamma_4) & c^2\Gamma_4 - s^2\Gamma_3 \end{bmatrix} \quad (1)$$

in the case of Fig. 1a) and

$$S_K = \frac{1}{1 - c^2\Gamma_3\Gamma_4} \begin{bmatrix} -s^2\Gamma_4 & c(1 - \Gamma_3\Gamma_4) \\ c(1 - \Gamma_3\Gamma_4) & -s^2\Gamma_3 \end{bmatrix} \quad (2)$$

for Fig. 1b), where  $c = \sqrt{1 - K}$ ,  $s = \sqrt{K}$  and  $\Gamma_i$  is the reflection coefficient at port  $i$ .

Typical reflection intensity responses are plotted in Figs. 2 and 3 for the Type I (Fig. 1a) and Type II mirrors (Fig 1b), respectively. The parameters used to compute these results were  $K_c = 0.02$ ,  $\alpha = 0$ , grating strength  $GS = (n_b - n_a)N_G/n_e = 3.92$ ,  $\lambda_0 = 1.5791\mu\text{m}$ ,  $N_3 = 10.25$ ,  $N_4 = 10$  and the parameter is  $N$ , ( $\sigma = \exp(-\alpha L)$ ).

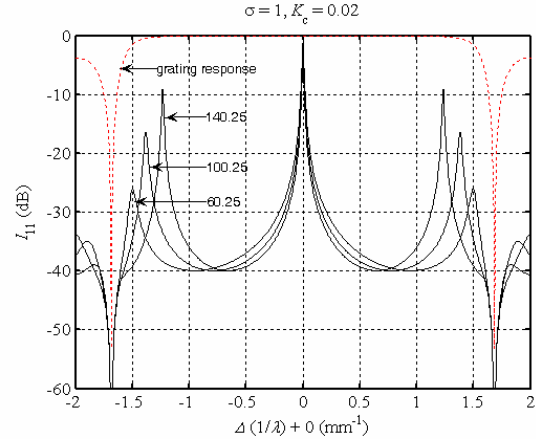


Fig. 3. Reflected intensity of the Type I mirror for three mode numbers. Also shown is the return loss of the gratings. The parameters are:  $N_G = 600$ ,  $n_a = 1.5098$ ,  $n_b = n_{eff} = 1.5$  ( $GS = 3.92$ ),  $K = 0.5$ ,  $K_c = 0.02$ ,  $\lambda_0 = 1.5791\mu\text{m}$ ,  $N_3 = 10.25$ ,  $N_4 = 10$ ,  $\alpha = 0$ . Multiply the abscissa by  $3 \times 10^2$  to obtain the detuning in GHz.

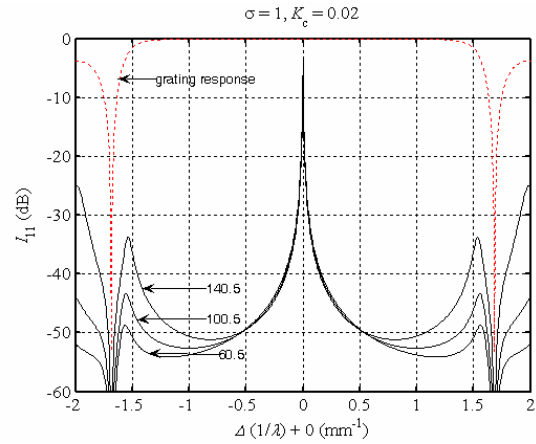


Fig. 4. Reflection response of the Type II mirror for three values of  $N$ ,  $N_3 = 10.5$ ,  $N_4 = 10$ ,  $\sigma = \exp(-\alpha L)$ . The remaining circuit parameters are identical to those given in the previous diagram.

### III. SELECTION RULES AND TUNABILITY

Selection rules govern the mode numbers  $N$ ,  $N_3$  and  $N_4$  to position the reflection peak at the design frequency  $f_0$ , at the center of the grating bandwidth, and provide constructive interference between the signal components reflected by the gratings at port 1. This interference is controlled by the phase shifts incurred by the coupled signals in the couplers and by the return phase of arms  $l_3$  and  $l_4$  which, in turn, depend on the lengths of these waveguides and on the index sequence used to fabricate the gratings. In our case the gratings consisted of *HLHL*.. index sequences with zero initial phase shift at the frontal interface.

Observe that in the Type I mirror the gratings are connected through the ring both clockwise and counter clockwise representing a phase shift difference of  $180^\circ$ . In the Type II mirror the gratings are connected first directly and secondly through the ring including an extra  $180^\circ$  phase shift incurred by crossing the coupler twice. This difference explains the nature of the selection rules for the mode numbers. One consequence is that the location of the coupler  $K$  in the Type II mirror can be shifted freely as long as  $N_3 + N_4 = INT + \frac{1}{2}$ . This does not apply to the Type I mirror. On the other hand the Type I mirror is insensitive to the value of  $K$  when  $N$  is varied to tune the device using e.g., a thermo-optic heater. In the Type II mirror this insensitivity applies only as long as the resonance peak is centered at  $f_0$ . The tuning sensitivity for the Type I mirror is indicated in Fig. 5. It decreases with increasing mode numbers but not linearly. The sensitivity of arms 3 and 4 are not the same because the return paths from them to port 1 are different. The corresponding sensitivities for Type I mirrors are similar except for the fact that the tuning sensitivity of arms 3 and 4 are the same. The tuning of neither mirror is sensitive to loss or to the value of  $K_c$ .

### IV. REFLECTION LOSS

Reflection loss results from waveguide loss and from leakage loss through finite gratings. The

former includes radiation loss from bent guides, scattering loss due to inclusions and wall imperfections, absorption loss, etc. The latter can

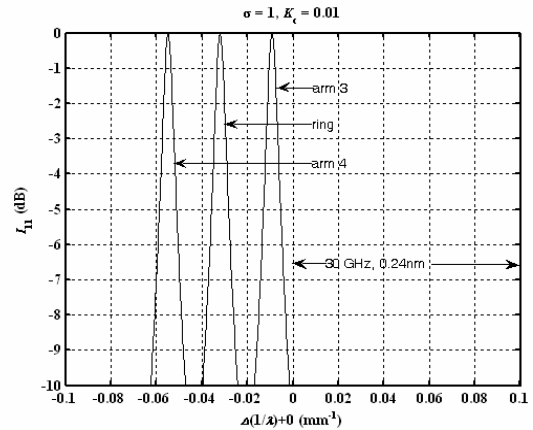


Fig. 5. Resonance shift caused by  $0.01\lambda$  length extension in the path indicated (Type I mirror).  $N = 100.25$ ,  $N_3 = 10$ ,  $N_4 = 10.25$ . The shift is insensitive to loss and the value of  $K_c$ .

be reduced by increasing the grating strength  $GS = (n_b - n_a)N_G/n_e$ . Fig. 6 plots reflection loss in Type I mirror due to grating leakage alone for three values of  $K_c$ . The corresponding  $RL$  for Type II mirrors are shown in Fig. 7. Observe that the  $RL$  is more than twice as large in the latter case. Reflection loss due to finite waveguide attenuation is plotted in Figs. 8 and 9 for Type I and Type II mirrors, respectively for a range  $0 < \alpha < 6\text{dB/cm}$ . Notice that the  $RL$  mounts sharply as  $K_c$  decreases. Once again the  $RL$  of Type II mirrors is more than twice the value of that of a Type I mirror.

### V. GROUP DELAY IN REFLECTION

The group delay in reflection:  $\tau_{11}$ , determines the overall round trip time of the laser signal which, in turn, determines its  $Q$  factor and the resonance bandwidth. The  $\tau_{11}$  characteristics of our mirrors display a single peak at resonance, with a maximum value depending on  $K_c$ , on the combined waveguide and leakage loss and on the mode numbers  $N$ ,  $N_3$  and  $N_4$ . Using the nominal mode numbers:  $N = 50$  and  $N_3 = N_4 = 10$  we obtained normalized group delays as listed in Table 1. These values are approximately

inversely proportional to the total path traveled in the mirror, i.e., when the sum  $N+N_3+N_4$  is increased the group delay in reflection is approximately proportionately decreased.

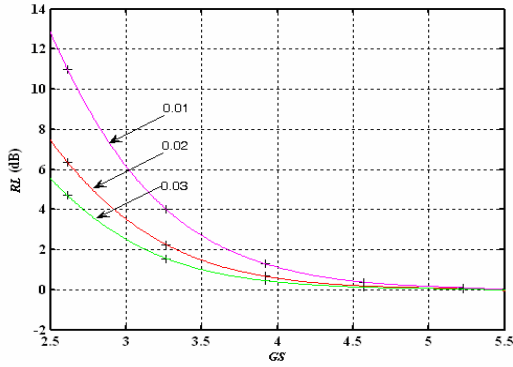


Fig. 6. Reflection loss at  $f_0$  due to finite grating length in Type I mirror. The  $RL$  does not depend on  $N$ . The abscissa is the grating strength  $GS = (n_a - n_b)N_G/n_e$ , the parameter is  $K_c$ , and  $\alpha = 0$ .

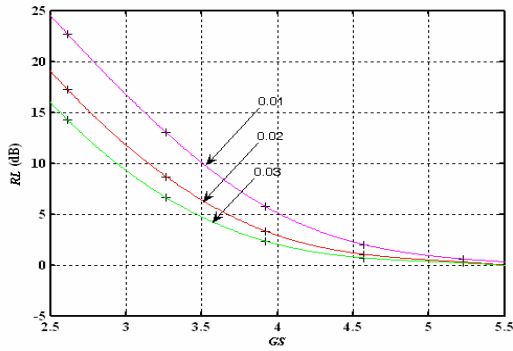


Fig. 7. Reflection loss at  $f_0$  due to finite grating length in Type II mirror. The  $RL$  does not depend on  $N$ . The abscissa is the grating strength  $GS = (n_a - n_b)N_G/n_e$ , the parameter is  $K_c$ , and  $\alpha = 0$ .

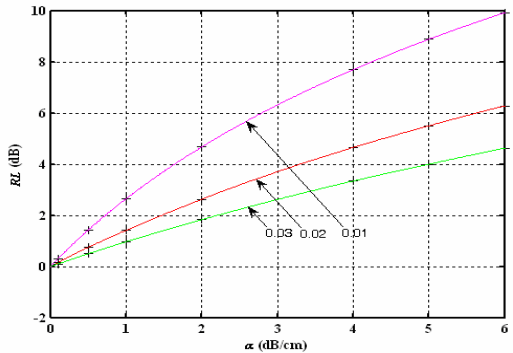


Fig. 8. Reflection loss at  $f_0$  due to finite  $\alpha$  in Type I mirror. The parameter is  $K_c$ , grating loss is negligible,  $N = 50.25$ ,  $N_3 = 10,25$ ,  $N_4 = 10$ .  $RL$  increases with  $N$ .

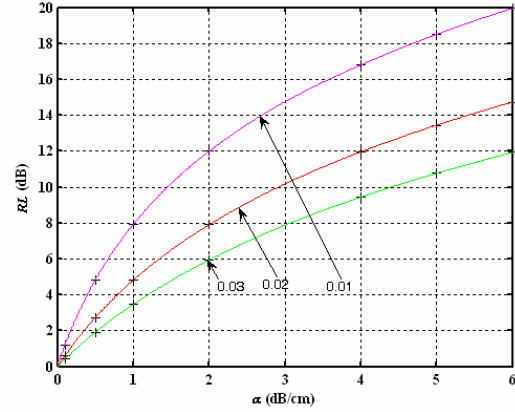


Fig. 9. Reflection loss at  $f_0$  due to finite  $\alpha$  in Type II mirror. The parameter is  $K_c$ , grating loss is negligible,  $N = 50.5$ ,  $N_3 = 10,25$ ,  $N_4 = 10$ . Increasing  $N$  increases the  $RL$ .

Table 1. Normalized group delay in reflection at resonance:  $\tau_{11}/\tau_0$ . Top row: Type I mirror, bottom row: Type II mirror.

	$K_c=0.01$	$K_c=0.03$	$K_c=0.05$
$\alpha=0.5\text{dB/cm}$ ( $\sigma=0.9997$ )	437	173.6	107.5
$\alpha=1.0\text{dB/cm}$ ( $\sigma=0.9994$ )	909	518	360
$\alpha=2.0\text{dB/cm}$ ( $\sigma=0.9988$ )	312.5	150	98
	497	350	270

The values in Table 1 were obtained for  $GS = 3.92$ . For larger  $GS$ , i.e., for smaller leakage loss, the group delay is larger as indicated by the rise of  $\tau_{11}/\tau_0$  with decreasing waveguide loss.

## VI. CONCLUSION

Two grating-assisted microring reflector configurations, suitable as laser mirrors have been analytically and numerically investigated. Their reflection characteristics have been compared and selection rules governing the proper mode numbers of the ring and the arms of the Bragg gratings for centering the reflection band were discussed. The effect on the reflected signal strength caused by waveguide loss as well as leakage loss from finite gratings has been computed. The effect of coupling on bandwidth and the rate of tunability have also been

documented. Comparisons between the mirrors allow for making a judicious selection.

### ACKNOWLEDGMENT

The support of the Spanish Ministry of Education project CICYT TEC2006-13273-C03-03/MIC and the Natural Sciences and Engineering Research Council of Canada are acknowledged.

### REFERENCES

- [1] I. Chremmos, and N. Uzunoglu, "Reflective properties of double-ring resonator system coupled to a waveguide," *IEEE Photon. Technol. Lett.*, vol. 17, no. 10, pp. 2110-2112, 2005.
- [2] Y. Chung, D.-G. Kim, and N. Dagli, "Widely tunable coupled-ring reflector laser diode," *IEEE Photon. Technol. Lett.*, vol. 17, no. 9, pp. 1773-1775, 2005.
- [3] J.K.S. Poon, J. Scheuer, and A. Yariv, "Wavelength-selective reflector based on a circular array of coupled microring resonators," *IEEE Photon. Technol. Lett.*, vol. 16, no. 5, pp. 1331-1333, 2004.
- [4] G.T. Paloczi, J. Scheuer, and A. Yariv, "Compact microring-based wavelength-selective inline optical reflector," *IEEE Photon. Technol. Lett.*, vol. 17, no. 2, pp. 390-392, 2005.
- [5] O. Schwelb, "Band-limited optical mirrors based on ring resonators: analysis and design," *J. Lightw. Technol.*, vol. 23, no. 11, pp. 3931-3946, 2005.
- [6] B. Liu, A. Shakouri, and J.E. Bowers, "Wide tunable double ring resonator coupled lasers," *IEEE Photon. Technol. Lett.*, vol. 14, no. 5, pp. 600-602, 2002.
- [7] C. Vázquez, S. Vargas, and J.M.S. Peña, "Design and tolerance analysis of a router with an amplified resonator and Bragg gratings," *Appl. Optics*, vol. 39, no. 12, pp. 1934-1940, 2000.
- [8] C. Vázquez, J. Montalvo, P.C. Lallana, and J.M.S. Peña, "Applications of recirculating optical configurations on filters and lasers," *Microtechnologies for the New Millennium 2005*, Proc. SPIE, vol. 5840, pp. 315-324, Sevilla (España) 9-11 May, 2005.
- [9] C. Vázquez, S. Vargas, and J.M.S. Peña, "Sagnac loop in Ring Resonators for Tuneable Optical Filters," *J. Lightw. Technol.*, vol. 23, no. 8, pp. 2555-2567, 2005.
- [10] C. Vázquez, S. Vargas, J.M.S. Peña, and P. Corredera, "Tunable Optical Filters Using Compound Ring Resonators for DWDM," *IEEE Photonics Technol. Lett.*, vol. 15, no. 8, pp. 1085-1087, 2003.
- [11] O. Schwelb, "Generalized analysis for a class of linear interferometric networks – Part II: simulations," *IEEE Trans. Microwave Theory Tech.*, vol. 46, no. 10, pp. 1409-1418, 1998.
- [12] G. Lenz, B.J. Eggleton, C.K. Madsen, and R.E. Slusher, "Optical delay lines based on optical filters," *IEEE J. Quantum Electron.*, vol. 37, no. 4, pp. 525-532, 2001.
- [13] B. Vizoso, C. Vázquez, R. Civera, M. López-Amo, and M.A. Muriel, "Amplified fiber-optic recirculating delay

lines," *J. Lightw. Technol.*, vol. 12, no. 2, pp. 294-305, 1994.

- [14] D.G. Rabus, M. Hamacher, U. Troppenz and H. Heidrich, "High- $Q$  channel-dropping filters using ring resonators with integrated SOAs," *IEEE Photonics Technol. Lett.*, vol. 14, no. 10, pp. 1442-1444, 2002.
- [15] O. Schwelb, and I. Frigyes, "Series-coupled microring resonator filters with embedded semiconductor optical amplifiers," *Microwave & Opt. Technol. Lett.*, vol. 42, no. 5, pp. 427-432, 2004.
- [16] I. Christiaens, D. Van Thourhout, and R. Baets, "Low-power thermo-optic tuning of vertically coupled microring resonators," *Elect. Lett.*, vol. 40, no. 9, pp. 560-561, 2004.